Decentralized Bilateral Aerial Teleoperation of Multiple UAVs – Part I: a Bottom-up Perspective

Paolo Robuffo Giordano
Max Planck Institute for Biological Cybernetics
Spemannstraße 38, 72076, Tübingen, Germany
Email: prg@tuebingen.mpg.de

***Abstract*—In this talk, we will review some recent advancements in the field of Aerial Teleoperation, i.e., how to bilaterally couple a single human operator with a remote fleet of semi-autonomous UAVs which 1) must keep some spatial formation and avoid inter- and obstacle- collisions, and 2) must collectively follow the human commands. The emphasis will be placed on the modeling and control tools needed for establishing such a non-conventional bilateral channel: in particular, we will study how to render the multi-UAV "slave side" a passive system w.r.t. the environment, and how to still enforce global connectivity maintenance despite limited sensing and loss of visibility because of occlusions.**

I. Introduction

For several applications like surveillance of large perimeters, search and rescue in disaster regions, and exploration of wide or unaccessible areas, the use of a group of simple robots rather than a single complex robot has proven to be very effective, and the problem of coordinating a group of agents has received a lot of attention by the robotics and control community over the last decade, see [16] for a survey. Indeed, such a fruitful interplay has resulted in significant advances in the mathematical formalization, theoretical analysis and actual realization of complex multi-robot systems for diverse applications, like exploration [10], coverage [24], cooperative transportation [5], formation control [1], distributed estimation [30] and sensing [15, 19]. Nevertheless, when the tasks become extremely complex and high-level cognitive-based decisions are required online (e.g., during exploration of very cluttered, dynamic and unpredictable environments for search and rescue applications), complete autonomy is still far from being reached and human's intervention/assistance is necessary. In this context, teleoperation systems, where a human operator commands a remote robot through a local interface, allow to exploit human's intelligence to solve tasks too complex for nowadays robots. Symmetrically, the enhancement of human perceptions and actions via a group of remote multiple robots, in order to operate rapidly and precisely at the macroscopic, microscopic, and planetary scales, constitutes a novel and challenging topic in the broad field of human–robot interfaces and telepresence applications.

In this talk, we will address the problem of establishing a *bilateral* teleoperation system for remotely controlling the motion of groups of Unmanned Aerial Vehicles (UAVs) in a decentralized way — that is, to achieve *Decentralized Bilateral Aerial Teleoperation*. Our focus will be placed on a fundamental problem: lay down an advantageous theoretical framework for remote *navigation* purposes, i.e., a necessary premise for any other specific objective, such as tele-exploration, -transport, or -manipulation. In our envisaged teleoperation system, the remote UAVs (the *slave-side* from now on) should possess some minimum level of local autonomy and act as a *group*, e.g., by maintaining some desired inter-distances and avoiding collisions by means of decentralized controllers. At the same time, the human operator, acting on the *master device*, should be in control of the overall group motion and receive, through haptic feedback, suitable cues informative enough of the remote robot/environment state. On top of this remote navigation layer, the group should still be allowed to perform additional local tasks by exploiting the internal slave side redundancy w.r.t. the master device commands.

Bilateral teleoperation of multiple UAVs presents several differences w.r.t. conventional teleoperation systems: first, there exists a structural *kinematic dissimilarity* between master and slave sides, i.e., the master possesses a limited workspace while the slave an unbounded one. Second, in a typical scenario, there is no physical contact with the environment since this would represent a dangerous situation (e.g., a crash) for the robots. Therefore, the interaction forces with the external world, such as contact forces, must be fabricated and, to some extent, a redefinition of standard concepts related to telepresence is required to properly assess the human operator immersiveness. In this respect, we recently presented some preliminary studies which are exploring the human perception point of view in these uncommon teleoperation scenarios [27, 28].

Furthermore, the slave-side possesses large motion redundancy w.r.t. the master-side because of the mismatch between the degrees of freedom (DOFs) of the master (usually in the range of 3–6), and the DOFs of the slave (in the range of $6N$ for N robots, when considered as rigid bodies). In addition to these issues, a proper design of a multi-UAV slave-side must also cope with the typical requirements of *decentralized sensing and control* for guaranteeing robustness to failures, achieving actual feasibility, and ensuring low computational load: roughly speaking, one should avoid the presence of any central sensing, communication or control unit in the network [4, 14, 16]. Finally, the design of the slave-side should accommodate for the presence of additional tasks independent

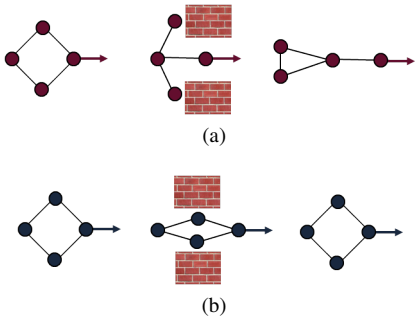

Fig. 1: Top: an illustrative picture of the *bottom-up* approach. Bottom: an illustrative picture of the *top-down* approach

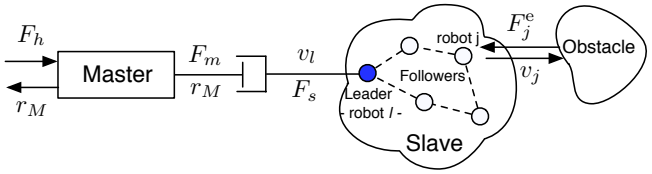

Fig. 2: The overall teleoperation system. From left to right: F_h is the human operator force applied to the master device; r_M is a velocity-like quantity which is almost proportional to the position of the haptic device; F_m is the control force applied to the master in order to provide haptic feedback; v_l is the velocity of the leader and F_s is a force applied to the leader to make it follow the desired velocity; finally v_j is the velocity of a generic j-th robot and F_j^{env} is its interaction force with the external environment (obstacles).

of the main navigation command received from the human operator. Therefore, stability w.r.t. time-varying interaction topology within the slave side network should also be granted.

In order to address these issues, we proposed in a recent work [8] a general framework for establishing a *bilateral teleoperation system* to control a remote group of UAVs in a *decentralized and flexible way*. This approach was named *bottom-up* because of the flexibility granted to the UAV fleet: the formation shape and topology could be autonomously adapted online via local split and join decisions due to sensing constraints and/or additional local tasks independent of the main navigation command. Figure 1(a) depicts an illustrative example of this scenario: a group of 4 agents splits some 'interaction links' in the proximity of an obstacle to actively reshape the formation and get over the narrow passage. Such flexible behavior was achieved by only requiring 1-hop information within the group, and a single communication link between the human operator and one of the robots (which was then referred to as the 'unique' leader). Tools from passivity theory were mainly exploited to characterize the stability of the (multi-)slave side and of the overall teleoperation system despite interaction with the environment and time-varying group topology. The human operator at the master side was feeling, through suitable force cues, the motion state of the fleet and the presence of (remote) obstacles. However, no synchronization among the UAVs actual velocities and the human/master velocity commands could be achieved because of a too conservative local damping action on the UAV side, and only hardware-in-the-loop simulations were reported.

Therefore, in a subsequent work [22], this approach was further extended in order to cope with the open points mentioned above: we devised a modified inter-agent damping strategy that allowed perfect velocity synchronization of the whole fleet w.r.t. the master commands, and presented the results of an extensive experimental evaluation obtained with 4 quadcopters teleoperated by a human operator. We also gave a rigorous characterization of the teleoperation steady-state behavior, both in terms of slave motion and force reflection on the master side for better illustrating the main features of our approach. However, we still did not explicitly consider any particular strategy for ensuring connectivity of the group during motion: a sub-group could still potentially detach from the component connected to the leader — a feature not desirable in all tasks. To cope with this problem, a further generalization was proposed in [21] to obtain a decentralized control action which could simultaneously enforce (i) obstacle/inter-robot collision avoidance and (ii) flexible connectivity maintenance of the group despite loss of sensing/visibility due to (too large) inter-robot distance and/or occluding obstacles.

We also note that a complementary stream of activities related to a *top-down* approach has been recently presented to the community, see [7, 9, 12]. The ideas behind them are briefly illustrated by Fig. 1(b): flexibility of the fleet is traded for a more rigid and pre-defined shape of the group, but still allowing local *reversible* deformations because of the interaction with the environment (obstacles). Imposing this kind of behavior to the slave-side finds applications in all those scenarios where maintaining a desired shape is mandatory, such as distributed monitoring, optimal placement for communication/exploration, and so on. Full details of these activities can be found in [6].

The rest of the paper will summarize the contributions of [8, 21, 22] to the *bottom-up* approach: as all the technical details and proofs can be found in these references, a (more) informal exposition style will be adopted in the following for facilitating the reading flow.

II. The Teleoperation System

In our scheme, depicted Fig. 2, the slave side consists of a group of N agents among which a *leader* is chosen (denoted by the subscript l). The motion of an agent depends on the motion of the locally surrounding agents and obstacles, by means of the action of *nonlinear elastic-like couplings*. The leader is a special agent that is also subject to the master control represented by the additional external force F_s. The remaining agents (not controlled by the master) are also referred to as *followers*. We let the spring coupling between a pair of agents to be broken and/or reestablished at anytime. In this way, we ensure high flexibility w.r.t. possible additional tasks, and adequate maneuverability within cluttered environments as the group shape does not result overly constrained. The design

and stability analysis of the slave side will be illustrated in the next Sect. III.

The velocity-like quantity r_M, (almost) proportional to the position of the master device, acts as velocity setpoint for the leader at the slave side thanks to the master/slave coupling force F_s. This allows to address the aforementioned master-slave kinematic dissimilarity. Conversely, the mismatch between r_M and the actual leader velocity v_l is transformed into the force F_m at the master side, in order to transmit to the user a feeling of the remote side (see Sect. IV). This force will be shown to carry information about the total number of agents in the group, and about the interaction with the surrounding environment since the followers at the slave side will influence the velocity of the leader.

Finally, passivity will be the leitmotif throughout the whole design and analysis phase. In fact, in order to ensure the stability of the system, our primary goal will be to design the master and slave side as passive systems joined by a passive interconnection. In this way the bilateral teleoperation system will be characterized by a stable behavior in case of interaction with passive environments and passive human users.

III. The Slave Side

The slave side consists of a group of N robots coupled together. In this Section we detail a control strategy for obtaining a flexible cohesive behavior of the group (i.e., allowing arbitrary split and join) and, at the same time, to avoid inter-robot and obstacle collisions. Every agent is modeled as a floating mass in $\mathbb{R}^3$, that is, an element storing kinetic energy:

$$\begin{cases} \dot{p}_i = F_i^a + F_i^e - B_i M_i^{-1} p_i \\ v_i = \frac{\partial \mathcal{K}_i}{\partial p_i} = M_i^{-1} p_i \end{cases} \qquad i = 1, \dots, N \qquad (1)$$

where $p_i \in \mathbb{R}^3$ and $M_i \in \mathbb{R}^{3\times 3}$ are the momentum and (positive definite) inertia matrix of agent i, respectively, $\mathcal{K}_i = \frac{1}{2} p_i^T M_i^{-1} p_i$ is the kinetic energy stored by the agent during its motion, and $B_i \in \mathbb{R}^{3\times 3}$ is a positive definite matrix representing an artificial damping added for asymptotically stabilizing the behavior of the agent[1]. Force $F_i^a \in \mathbb{R}^3$ represents the interaction of agent i with the other agents and will be designed in the following, while $F_i^e \in \mathbb{R}^3$ represents the interaction of agent i with the 'external world', i.e., the environment (obstacles) and the master side through the teleoperation channel (Sect. V). Finally, $v_i \in \mathbb{R}^3$ denotes the velocity of the agent, and $x_i \in \mathbb{R}^3$ indicates the position of the agent with $\dot{x}_i = v_i$.

Definition 1. *Two agents i and j are defined as being* neighbors *if and only if these two conditions are met:* i) *their inter-distance $d_{ij} = \|x_i - x_j\|$ is less than $D \in \mathbb{R}^+$, and* ii) *their* connection *state is set to* `true`.

The first condition models a generic limited range capability of onboard sensors and/or communication complexity of the robot network. In the second condition, the connection state may depend on arbitrary criteria and is taken as an exogenous binary signal. This allows to accommodate for additional task requirements independent from the main navigation task (e.g., separation of the fleet in different logical subgroups in order to accomplish different objectives). The connection state can also account for sensors not able to provide the mutual position even if $d_{ij} < D$ (e.g., visibility sensors such as cameras). According to this definition, we denote with $\mathcal{N}_i$ the set of neighbors of i. Since the relationship is symmetrical, $j \in \mathcal{N}_i \Rightarrow i \in \mathcal{N}_j$. Two agents i and j are said to *join* if they become neighbors and, conversely, are said to *split* if they become non-neighbors. Finally, we also denote with $\mathcal{G}(t) = (\mathcal{V}, \mathcal{E}(t))$ the undirected graph induced by this neighboring relationship where the vertices $\mathcal{V}$ represent the agents and $\mathcal{E}(t) = \{(i,j) \in \mathcal{V} \times \mathcal{V} \,|\, j \in \mathcal{N}_i\}$.

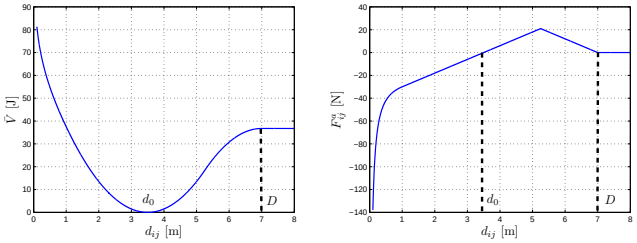

Fig. 3: The shape of the interagent potential as a function of the distance (left), and the corresponding coupling force (right)

The interaction forces acting among pairs of neighboring agents are modeled as nonlinear elastic elements characterized by an energy function $\bar{V}(d_{ij})$, where $d_{ij} = \|x_i - x_j\|$ is the relative distance between agents i and j. As proposed in [25], such energy storing elements are described by

$$\begin{cases} \dot{x}_{ij} = v_{ij} \\ F_{ij}^a = \frac{\partial V(x_{ij})}{\partial x_{ij}} \end{cases} \qquad (2)$$

where $x_{ij} = x_i - x_j$, v_{ij}, $F_{ij}^a \in \mathbb{R}^3$ are, respectively, the state, the input, and the output (i.e., the generated force) of the virtual spring.

Let $d_0 < D$ be a desired distance between the agents: the potential function $\bar{V}(d_{ij})$ is designed such that: if $d_{ij} < d_0$ a repulsive force is generated; if $d_{ij} = d_0$ a null force is produced; and if $d_0 < d_{ij} \leq D$ an attractive force is computed. We also assume that, if $d_{ij} > D$, a null force is generated since, in this case, $j \notin \mathcal{N}_i$. Notice that, according to the previous definitions, it is $F_{ij}^a = -F_{ji}^a$. A possible potential function $\bar{V}(d_{ij})$ with such a desired behavior is shown in Fig. 3. Note that the shape of the potential goes to infinity as d_{ij} approaches zero for providing an effective inter-agent repulsive force[2].

[1] This can also represent typical physical phenomena such as wind/atmospehere drag for aerial robots, or hydrodynamic drag for underwater robots.

[2] In general, any lower bounded potential (e.g., the one proposed in [23]) having similar features would be a suitable choice.

The coupling force of agent i is then

$$F_i^a = \sum_{j\in\mathcal{N}_i} F_{ij}^a := \sum_{j\in\mathcal{N}_i} \frac{\partial \bar{V}}{\partial d_{ij}} \frac{\partial d_{ij}}{\partial x_{ij}} = \sum_{j\in\mathcal{N}_i} \frac{\partial \bar{V}}{\partial d_{ij}} \eta_{ij}. \quad (3)$$

We note that the interaction force F_i^a can be computed by agent i in a decentralized way. In fact, the computation is based on the shape of the inter-agent potential (which is known from the design phase), and on the distance and bearing or agent j w.r.t. agent i.

In order to write the overall agent/spring dynamics (slave-side) in a compact form, define $p = (p_1^T, \dots, p_N^T)^T \in \mathbb{R}^{3N}$, $B = diag(B_i) \in \mathbb{R}^{3N\times 3N}$, $x = (x_{12}^T, \dots, x_{1N}^T, x_{23}^T, \dots, x_{2N}^T, \dots, x_{N-1N}^T)^T \in \mathbb{R}^{\frac{3N(N-1)}{2}}$ and $F^e = (F_1^{eT}, \dots, F_N^{eT})^T \in \mathbb{R}^{3N}$, and let $\mathcal{I}_\mathcal{G}(t) \in \mathbb{R}^{N\times\frac{N(N-1)}{2}}$ be the incidence matrix of the graph $\mathcal{G}(t)$ with the edge numbering and orientation induced by the entries of vector x. Notice that $\mathcal{I}_\mathcal{G}(t)$ has a constant size despite of the time-varying nature of $\mathcal{G}(t)$. Indeed, $j \notin \mathcal{N}_i$ will result in a column of all zeros for $\mathcal{I}_\mathcal{G}(t)$ in correspondence of the edge (i, j). It is then possible to model the slave side as a mechanical system described by:

$$\begin{cases} \begin{pmatrix} \dot{p} \\ \dot{x} \end{pmatrix} = \left[\begin{pmatrix} 0 & \mathcal{I}(t) \\ -\mathcal{I}^T(t) & 0 \end{pmatrix} - \begin{pmatrix} B & 0 \\ 0 & 0 \end{pmatrix} \right] \begin{pmatrix} \frac{\partial H}{\partial p} \\ \frac{\partial H}{\partial x} \end{pmatrix} + GF^e \\ v = G^T \begin{pmatrix} \frac{\partial H}{\partial p} \\ \frac{\partial H}{\partial x} \end{pmatrix} \end{cases} \quad (4)$$

where

$$H = \sum_{i=1}^{N} \mathcal{K}_i + \sum_{i=1}^{N-1} \sum_{j=i+1}^{N} V(x_{ij}) \quad (5)$$

is the total energy of the system, $\mathcal{I}(t) = \mathcal{I}_\mathcal{G}(t) \otimes I_3$, and $G = \left((I_N \otimes I_3)^T \quad 0^T\right)^T$, with I_3 and I_N being the identity matrices of order 3 and N respectively, 0 representing a null matrix of proper dimensions, and $\otimes$ denoting the Krönecker product.

Proposition 1. *Assuming $\mathcal{I}(t) = const$, i.e., no splits and joins are taking place, system (4) is passive with respect to the input/output pair (F^e, v) with storage function H.*

Proof: See [8]. ∎

Since (4) is a passive system, its interaction with any passive environment will still preserve passivity. This easily allows to include in inputs F_i^e in (1) an obstacle avoidance action. Indeed, as usual in applications involving mobile agents in unknown environments, we assume that, when they are detected, obstacles are treated as repulsive potentials producing a force that vanishes if the robot is far enough and grows as the robot comes closer to the obstacle. Such potentials can also be modeled as virtual springs, that is, passive systems, and their action is considered to be embedded in the terms F_i^e.

Having established passivity of the slave-side with a constant interaction graph topology $\mathcal{G} = const$, we now analyze the general case of a time-varying $\mathcal{G}(t)$ because of the join and split decisions of Def. 1.

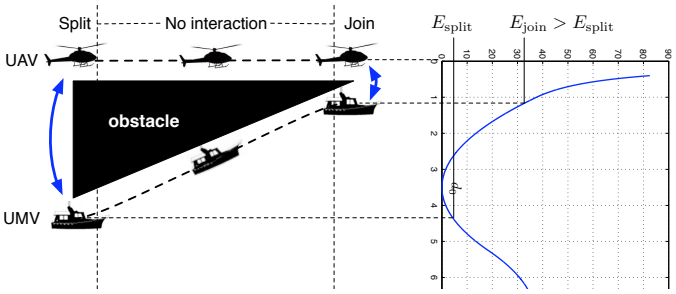

Fig. 4: When the agents split the energy E_{split} is stored in the spring, while when they join the energy $E_{\text{join}} > E_{\text{split}}$ is needed to implement the new desired coupling. In this case, without proper strategies, an amount $E_{\text{join}} - E_{\text{split}} > 0$ of energy would be introduced into the system, thus violating passivity.

Proposition 2. *If two agents split then passivity of (4) is preserved.*

Proof: See [8]. ∎

A join decision, on the other hand, can lead to a violation of passivity: when two agents i and j join, they instantaneously switch from a state characterized by no interaction, to the inter-agent interaction represented by Eq. (2). Some extra energy can be produced during the join procedure, possibly threatening the passivity of the system. In fact, in the general case, the relative distance of two agents at the join decision can be different from their relative distance at the split decision, and this can result in a non passive behavior: the illustrative example of Fig. 4 shows this situation.

To remedy this problem and implement the join procedure in a passive way, we propose to keep track of the energy dissipated by each agent: to this end, we introduce a local variable $t_i \in \mathbb{R}$, called *tank*, along with an associated energy function $T_i = \frac{1}{2}t_i^2$ for storing the energy dissipated by the agent. This energy reservoir can then be used for compensating excess of energy in the slave side and, thus, for implementing join decisions without violating the passivity of the system. Using Eq. (1), the energy dissipated by agent i because of the damping is

$$D_i = p_i^T M_i^{-T} B_i M_i^{-1} p_i. \quad (6)$$

Considering the tank variables, we then propose to adopt the following extended dynamics for the agents and elastic elements:

$$\begin{cases} \dot{p}_i = F_i^a + F_i^e - B_i M_i^{-1} p_i \\ \dot{t}_i = (1-\beta_i)\left(\alpha_i \frac{1}{t_i} D_i + \sum_{j=1\dots N, j\neq i} w_{ij}^T F_{ij}^a\right) + \beta_i c_i \\ y_i = \begin{pmatrix} M_i^{-1} p_i \\ t_i \end{pmatrix} \end{cases} \quad (7)$$

$$\begin{cases} \dot{x}_{ij} = v_{ij} - (1-\beta_i) w_{ij} t_i + (1-\beta_j) w_{ji} t_j \\ F_{ij}^a = \dfrac{\partial V(x_{ij})}{\partial x_{ij}} \end{cases} \quad (8)$$

The quantity $\alpha_i \in \{0,1\}$ is a design parameter that disables/enables the storage of D_i, the energy dissipated by the system. The quantity $\beta_i \in \{0,1\}$ is a design parameter which allows to switch the behavior of the tank element from a *storage mode* (i.e., the energy dissipated by the agent is stored) to a *consensus mode* (i.e., a consensus algorithm is run among the tanks). The role of inputs $w_{ij} \in \mathbb{R}^3$ is to allow for an energy exchange among the tank energy T_i and the elastic elements $V(x_{ij})$.

As explained in [8], it is then possible to run a decentralized `PassiveJoin` Procedure which allows to safely (i.e., passively) implement join decisions: in brief, whenever a join decision is producing extra energy $\Delta E > 0$ because of situations conceptually similar to Fig. 4, the energy in the tanks of agents i and j is exploited to account for this energy excess. In case $T(t_i)$ and (T_j) is not sufficient to cover for $\Delta E > 0$, a consensus algorithm is run on the fleet to level all tank energies and possibly increase the local reservoirs of agents i and j. When this is not yet enough, an extra damping action is set on agents i and j to slow down their motion and quickly refill the tanks.

The behavior of the slave side when the `PassiveJoin` Procedure is implemented can be described by the following system:

$$\begin{cases} \begin{pmatrix} \dot{p} \\ \dot{x} \\ \dot{t} \end{pmatrix} = \left[\begin{pmatrix} 0 & \mathcal{I}(t) & 0 \\ -\mathcal{I}^T(t) & 0 & \Gamma^T \\ 0 & -\Gamma & 0 \end{pmatrix} - \right. \\ \left. - \begin{pmatrix} B & 0 & 0 \\ 0 & 0 & 0 \\ -(I-\beta)\alpha P B & 0 & 0 \end{pmatrix} \right] \begin{pmatrix} \frac{\partial \mathcal{H}}{\partial p} \\ \frac{\partial \mathcal{H}}{\partial x} \\ \frac{\partial \mathcal{H}}{\partial t} \end{pmatrix} + \begin{pmatrix} 0 \\ 0 \\ \beta c \end{pmatrix} + G F^e \\ v = G^T \begin{pmatrix} \frac{\partial \mathcal{H}}{\partial p} \\ \frac{\partial \mathcal{H}}{\partial x} \\ \frac{\partial \mathcal{H}}{\partial t} \end{pmatrix} \end{cases} \tag{9}$$

where

$$\mathcal{H} = \sum_{i=1}^{N} \mathcal{K}_i + \sum_{i=1}^{N-1} \sum_{j=i+1}^{N} V(x_{ij}) + \sum_{i=1}^{N} T_i \tag{10}$$

is the augmented total energy of the system. The matrix $\Gamma \in \mathbb{R}^{N \times \frac{3N(N-1)}{2}}$ represents the interconnection among tanks and elastic elements mediated by inputs w_{ij}. Finally, $\alpha = diag(\alpha_i)$ and $\beta = diag(\beta_i)$ are matrices containing the mode switching parameters, $P = diag(\frac{1}{t_i} p_i^T M_i^{-T})$, $t = (t_1, \ldots, t_N)^T$, and $c = (c_1, \ldots, c_N)^T$.

Proposition 3. *The system represented in Eq. (9) is passive with respect to the input/output pair (F^e, v) with storage function $\mathcal{H}$.*

Proof: See [8]. ∎

IV. The Master Side

We assume the master to be a generic mechanical system described by the following Euler-Lagrange equations:

$$M_M(x_M)\ddot{x}_M + C(x_M, \dot{x}_M)\dot{x}_M + D\dot{x}_M = F_M \tag{11}$$

where M_M represents the inertia matrix, $C(x_M, \dot{x}_M)\dot{x}_M$ is a term representing the centrifugal and Coriolis effects and where we assume that gravity is locally compensated. The variables x_M and $v_M := \dot{x}_M$ represent the position and the velocity of the end-effector. By introducing a scaling into the strategy proposed in [3, 13], it is possible to render the master passive with respect to the pair $(F_M,\, r_M)$ where

$$r_M = \rho v_M + \rho \lambda x_M, \qquad \rho > 0,\ \lambda \in (0,\, \lambda_{\max}]. \tag{12}$$

By properly choosing the design parameters ρ and λ it is then possible to make negligible the contribution related to v_M (by choosing a small ρ), and to make the second term proportional to the position with a desired scaling factor K (by choosing $\lambda = \frac{K}{\rho}$). Therefore, one can exploit the position-like variable r_M in order to passively couple the master side with the remote slave side through the power port $(F_M,\, r_M)$.

V. Master-Slave Interconnection

Without loss of generality, suppose that agent 1 is chosen as the leader. It is possible to decompose $F_1^{\text{e}} = F_s + F_1^{\text{env}}$, where F_1^{env} is the component of the force due to the interaction with the external environment (obstacles) and F_s is the component due to the interaction with the master side. Similarly, we can decompose F_M in Eq. (11) as $F_M = F_m + F_h$, where F_h is the component due to the interaction with the user and F_m is the force acting on the master because of the interaction with the slave.

For achieving the desired teleoperation behavior, master and slave sides are joined using the following interconnection:

$$\begin{cases} F_s = -b_T(v_1 - r_M) \\ F_m = b_T(v_1 - r_M) \end{cases} \tag{13}$$

where $b_T > 0$ is a design parameter. This is equivalent to joining the master and the leader using a damper which generates a force proportional to the difference of the two velocity-like variables of the master and the leader. Since r_M is "almost" the position of the master, the force fed back to the master and the control action sent to the leader are the desired ones. The complete teleoperation system, represented in Fig. 2, consists of the interconnection of a passive master side, a passive interconnection and a passive slave side. Recalling that the interconnection of passive systems is again passive [26], we can conclude that the teleoperation system is passive w.r.t. external actions (human force F_h and environment). We also note that, although not explicitly considered, passivity of the teleoperation system can be easily enforced also in presence of communication delays between local and remote sites using any of the techniques developed in conventional teleoperation settings as, e.g., wave variables [17].

VI. Decentralized Velocity Synchronization

The approach proposed so far allows to obtain a great flexibility of the fleet that can autonomously handle the navigation in cluttered environments. The agents can decide necessary split or join maneuvers without direct human intervention while preserving passivity of the overall teleoperation system.

At the same time, the human operator can control the overall fleet motion by regulating the leader velocity through F_s in Eq. (13), and by receiving, through F_m, a force cue informative of the agent motion status. However, as explained in [22], the presence of a continuous local damping action B_i can be too conservative: the dissipated energy keeps replenishing the tank T_i until its maximum value $\bar{T}_i$ but is, otherwise, wasted. On the other side, it is possible to prove that this continuous dissipation "brakes" the agents and prevents them from achieving velocity synchronization with the r_m variable of the master. At steady-state, the agents will synchronize to a fraction of the commanded r_m depending on the magnitude of their local damping B_i.

A possible workaround is to replace the constant damping term B_i in (7) with a control action F_i^d defined as:

$$F_i^d = -B_i(t_i) M_i^{-1} p_i \tag{14}$$

where

$$B_i(t_i) = \begin{cases} 0 & \text{if} \quad T(t_i) \geq \bar{T}_i \\ \bar{B}_i & \text{if} \quad T(t_i) < \bar{T}_i \end{cases} \tag{15}$$

with $\bar{B}_i$ a positive definite matrix. The term F_i^d represents a variable damping action and, analogously to before, its associated dissipated power D_i is injected back into the tank T_i. However, this dissipation takes place only when a tank refill is necessary, as for example after an energy consuming join maneuver. This ensures that the tanks are timely refilled but avoids the dissipation of energy that could not be stored and which would constantly "brake" the agent. The control parameter α_i in (7) is not needed any longer because its role is played by the variable damping strategy in Eq. (15). Similarly, we can also disregard the input c_i and the control parameter β_i.

An additional control action F_i^s is added to (7) in order to synchronize the velocity of the agents

$$F_i^{\mathrm{s}} = -b \sum_{j \in \mathcal{N}_i} (v_i - v_j). \tag{16}$$

This action is physically equivalent to a damper between neighboring agents. Since also this force is agent-wise symmetric, the interactions among the agents can still be modeled by the same undirected graph $\mathcal{G} = (\mathcal{V}, \mathcal{E}(t))$ exploited for the inter-agent couplings (2). Considering these modifications, the new dynamics of the slave side becomes:

$$\begin{cases} \begin{pmatrix} \dot{p} \\ \dot{x} \\ \dot{t} \end{pmatrix} = \left[\begin{pmatrix} 0 & \mathcal{I} & 0 \\ -\mathcal{I}^T & 0 & \mathcal{I}_\gamma \\ 0 & -\mathcal{I}_\gamma^T & 0 \end{pmatrix} - \begin{pmatrix} \mathcal{L}+B & 0 & 0 \\ 0 & 0 & 0 \\ -PB & 0 & 0 \end{pmatrix} \right] \nabla H + G F^E \\ v = G^T \nabla H \end{cases} \tag{17}$$

with now B representing the block diagonal matrix whose elements are the variable dampers of Eq. (15). The matrix $\mathcal{L} = bL_{\mathcal{G}} \otimes I_3$, where $L_{\mathcal{G}}$ is the positive semidefinite Laplacian matrix of the graph $\mathcal{G}$, derives from the control action reported in Eq. (16), which is formally equivalent to a consensus algorithm among velocities (see, e.g., [20]). The vector $F^E = (F_1^e, F_2^e, \ldots, F_N^e)$ indicates the external forces acting on the agents and H is the same lower bounded energy function given in Eq. (10)

Proposition 4. *The slave side described in Eq. (17) is passive with respect to the pair of variables (F^e, v) and the storage function reported in Eq. (10)*

Proof: See [22]. ■

It is then possible to formally characterize the steady state behavior of the teleoperation system under this new damping strategy. The following result characterizes the behavior of the system in *free motion*.

Proposition 5. *Let the master be kept at a constant configuration $(x_m, \dot{x}_m) \equiv (\bar{x}, 0)$ by a suitable human force F_h whose steady-state value will be determined in the following. Suppose also that (i) $F_i^e = 0$ for $i = 2, \ldots, N$ and $F_1^{env} = 0$ (agents moving in free motion), (ii) $B_i(t_i) = 0$ and $\mathcal{I}_\gamma = 0$ (tanks are full and no energy exchange takes place between tanks and springs), and (iii) the graph $\mathcal{G}$ is connected. Then, at steady-state:*

1) *the velocities of the agents synchronize to $K\bar{x}$;*
2) *the relative distances among the agents remain constant;*
3) *no force must be provided by the user, i.e., $F_h = 0$.*

Proof: See [22]. ■

During a normal operation, the human user will perceive a non-null force cue because of the mismatch between the commanded r_m and v_1. However, as shown above, this force cue will eventually vanish at steady-state informing her/him about the reached velocity synchronization among the agents.

We now focus on an opposite steady-state condition involving a *clamped slave*, i.e., with the agents obstructed by the environment (obstacles). We will again characterize the resulting force cue displayed to the human user.

Proposition 6. *Let the master be kept at a constant configuration $(x_m, \dot{x}_m) \equiv (\bar{x}, 0)$ by a suitable human force F_h whose steady-state value will be determined in the following. Suppose also that (i) there exist suitable environmental forces F_i^e, for $i = 2 \ldots N$, and F_1^{env} that keep $p \equiv v \equiv 0$ for all agents despite the human command (clamped slave), and (ii) $\mathcal{I}_\gamma = 0$ (no energy exchange takes place between tanks and springs). Then, at steady-state:*

1) *the relative distances among the agents remain constant;*
2) *the force provided by the human operator is $F_h = -F_1^{env} - \sum_{i=2}^{N} F_i^e$ (static reflection of the environmental forces).*

Proof: See [22]. ■

VII. Decentralized Connectivity Maintenance

As a final extension to our framework, we present a passive decentralized strategy that allows to enforce connectivity maintenance of the group at all times during the fleet motion. Generally speaking, in literature two classes of decentralized connectivity maintenance approaches are present: *i)* the *conservative* methods, which aim at preserving the initial graph topology during the task [2, 11, 18], and *ii)* the *flexible*

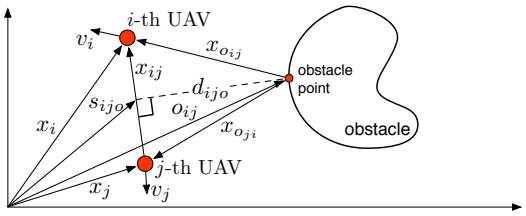

Fig. 5: The agents i and j and their closest obstacle point with the main symbols defined in the paper.

approaches, which allow to switch anytime among any of the connected topologies. These usually produce local control actions aimed at keeping (a decentralized estimate of) λ_2, the second smallest eigenvalue of the graph Laplacian, positive over time [29, 31]. In [21], we proposed a strategy which can be considered as an extension of the latter approaches, and which will be summarized in the following.

We start by slightly modifying the agent dynamics (7) as

$$\begin{cases} \dot{p}_i = F_i^\lambda + F_i^e - w_i t_i - B_i M_i^{-1} p_i \\ \dot{t}_i = \alpha_i \frac{1}{t_i} D_i + w_i^T v_i \\ y_i = \begin{pmatrix} v_i^T & t_i \end{pmatrix}^T \end{cases} \tag{18}$$

where now the interaction of agent i with the other agents and surrounding environment (obstacles) is embedded into $F_i^\lambda \in \mathbb{R}^3$, and input w_i exchanges energy among the tank and the agent kinetic energy. We also replace the neighboring definition of Def. 1 by the following

Definition 2. *Agents i and j are* neighbors *if and only if: i) their relative distance d_{ij} is less than $D \in \mathbb{R}^+$ (the sensing range) and larger than $d_{\min} \in [0, D)$ (the safety range), ii) their line-of-sight is not occluded by an obstacle, and iii) neither i nor j are closer than $d_{\min}$ to any other agent.*

The two latter conditions distinguish our work from most of the past literature on connectivity maintenance and are crucial for embedding both obstacle and inter-agent/collision avoidance within a unified *connectivity-preserving* action[3].

With reference to Fig. 5, let again $x_{ij} = x_i - x_j \in \mathbb{R}^3$ represent the relative position of agent i w.r.t. agent j and $x_{\mathrm{R}} = (x_{12}^T \ \dots \ x_{1N}^T \ x_{23}^T \ \dots \ x_{2N}^T \ \dots \ x_{N-1N}^T)^T \in \mathbb{R}^{\frac{3N(N-1)}{2}}$. We also let $\mathcal{O}_i$ be a set containing all the obstacle points sensed by agent i plus a fictitious point o_∞ at a distance greater than D from any agent (i.e., at *infinity*). If $j \in \mathcal{N}_i$, we let o_{ij} be the closest point in $\mathcal{O}_i \cup \mathcal{O}_j$ to the segment (*line-of-sight*) joining agent i and agent j. Notice that if $\mathcal{O}_i \cup \mathcal{O}_j$ does not contain any sensed obstacle point, then we define $o_{ij} = o_\infty$. We also set $o_{ij} = o_\infty$, by convention, whenever $j \notin \mathcal{N}_i$. By letting $x_{o_{ij}} = x_i - o_{ij}$ represent the relative position of agent i w.r.t. obstacle point o_{ij}, and $x_{o_i} = (x_{o_{i1}}^T \dots x_{o_{ik}}^T \dots x_{o_{iN}}^T)^T \in \mathbb{R}^{3(N-1)}$, $k \neq i$, we can collect all such relative positions for all the N robots into a unique vector $x_{\mathrm{O}} = (x_{o_1}^T \dots x_{o_N}^T)^T \in \mathbb{R}^{3N(N-1)}$. Analogously to the definition of x_{O}, we also collect all the obstacle point positions o_{ij} into a cumulative vector $o = (\dots, o_{i1}^T, \dots, o_{ij}^T \dots, o_{iN}^T \dots) \in \mathbb{R}^{3N(N-1)}$, with $i = 1, \dots, N$ and $j \neq i$, and let $v_o = \dot{o}$ be the obstacle point velocities seen from the corresponding agents[4].

Finally, we define a suitable scalar lower-bounded potential $V^\lambda(x_{\mathrm{R}}, x_{\mathrm{O}}) \in \mathbb{R}^+$ whose exact shape will be detailed in the following. For now, V^λ is meant to be a generic potential function accounting for connectivity maintenance, inter-agent collision avoidance, and obstacle avoidance for all the N robots in the group. This allows again to model the inter-agent and environment interaction as a nonlinear elastic element whose potential energy function is V^λ and whose gradient $\frac{\partial V^\lambda}{\partial (x_R \, x_O)}$ drives the agents toward the desired behavior. The potential V^λ is designed in such a way that x_{ij} and $x_{o_{ij}}$ do not contribute to its variation w.r.t. the agent position x_i when $j \notin \mathcal{N}_i$; thus, the control action implemented on agent i will take the (decentralized) form:

$$F_i^\lambda = \sum_{j \in \mathcal{N}_i} \left(\frac{\partial V^\lambda}{\partial x_{o_{ij}}} + \frac{\partial V^\lambda}{\partial x_{ij}} \right). \tag{19}$$

By defining $p = (p_1^T \ \dots \ p_N^T)^T \in \mathbb{R}^{3N}$, $t = (t_1 \ \dots \ t_N)^T \in \mathbb{R}^N$, $B = diag(B_i)$, and $F^e = (F_1^{eT} \ \dots \ F_N^{eT})^T \in \mathbb{R}^{3N}$, and by noting that $\dot{x}_{ij} = v_i - v_j$, we can then model the overall *slave-side* as a mechanical system described by:

$$\begin{cases} \begin{pmatrix} \dot{p} \\ \dot{x}_R \\ \dot{x}_O \\ \dot{t} \end{pmatrix} = \left[\begin{pmatrix} 0 & \mathcal{I} & -\mathbb{I} & \Upsilon \\ -\mathcal{I}^T & 0 & 0 & 0 \\ \mathbb{I}^T & 0 & 0 & 0 \\ -\Upsilon^T & 0 & 0 & 0 \end{pmatrix} - \begin{pmatrix} B & 0 & 0 & 0 \\ 0 & 0 & 0 & 0 \\ 0 & 0 & 0 & 0 \\ -\alpha P B & 0 & 0 & 0 \end{pmatrix} \right] \nabla \mathcal{H} \\ \quad + G \begin{pmatrix} F^{\mathrm{e}} \\ v_o \end{pmatrix} \\ \begin{pmatrix} v \\ F^o \end{pmatrix} = G^T \nabla \mathcal{H} \end{cases} \tag{20}$$

where

$$\mathcal{H} = \sum_{i=1}^{N} (\mathcal{K}_i + T_i) + V^\lambda \in \mathbb{R}^+ \tag{21}$$

represents the total energy of the system and $\nabla \mathcal{H} = \left(\frac{\partial^T \mathcal{H}}{\partial p} \frac{\partial^T \mathcal{H}}{\partial x_R} \frac{\partial^T \mathcal{H}}{\partial x_O} \frac{\partial^T \mathcal{H}}{\partial t} \right)^T$. Moreover, $\mathcal{I} = \mathcal{I}_\mathcal{G} \otimes I_3$, $\mathbb{I} = I_N \otimes \mathbf{1}_{N-1}^T \otimes I_3$, $\Upsilon = diag(-w_i)$, and $G = \begin{pmatrix} I_N \otimes I_3 & 0 & 0 \\ 0 & 0 & -\mathbb{I} \end{pmatrix}^T$, with $\mathcal{I}_\mathcal{G}$ being the incidence matrix of the graph $\mathcal{G}$ whose edge numbering is induced by the entries of the vector x_R, I_3 and I_N being the identity matrices of order 3 and N respectively, $\mathbf{1}_{N-1}$ a column vector of all ones of dimension $N-1$, 0 representing a null matrix of proper dimensions, and $\otimes$ denoting the Krönecker product. Furthermore, $P = diag(\frac{1}{t_i} p_i^T M_i^{-T})$, $\alpha = diag(\alpha_i)$, and $v \in \mathbb{R}^{3N}$ and $F^o \in \mathbb{R}^{3N(N-1)}$ are the conjugate power variables associated to F^e and v_o, respectively: the system exchanges energy through the port (F^e, v)

[3]Although not commonly considered in the literature, enforcing a minimum inter-agent safe distance $d_{\min}$ is also relevant in many practical circumstances involving local sensing such as, e.g., limited focusing range of on-board cameras, occlusions due to too close agents, or a generic safe distance to prevent dangerous collisions.

[4]In fact, even though the obstacles are supposed to be fixed in space, the obstacle points move as the agents move.

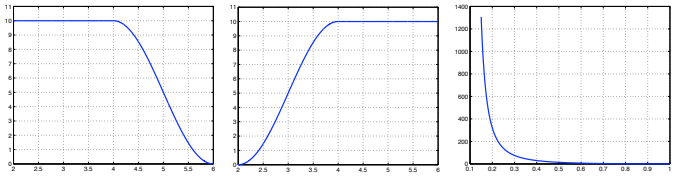

(a) (b) (c)

Fig. 6: The shape of a_{ij} (left), b_{ij} (equiv. c_{ij}) (center), and $V^{\lambda}(\lambda_2)$ (right).

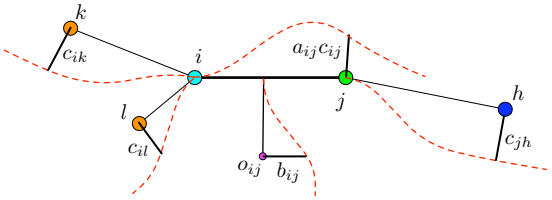

Fig. 7: Graphical representation of the terms contributing to $A_{ij} = a_{ij}b_{ij}c_{ij}c_{ik}c_{il}c_{jh}$. In this example k and l are the neighbors of i, h is the neighbor of j, and o_{ij} is the closest obstacle point to the segment joining i and j.

with the external world, and through the port (v_o, F^o) with the obstacles, which are considered as a passive system.

Proposition 7. *The slave side is passive with respect to the storage function reported in Eq. (21).*

Proof: See [21]. ■

A. The connectivity potential V^{λ}

Inspired by [29], we encode the connectivity relationship of Def. 2 into the weights of the links joining neighboring agents. To this end, let $A \in \mathbb{R}^{N\times N}$ be the adjacency matrix associated to the graph $\mathcal{G}$: each element $A_{ij} \in \mathbb{R}^{+}$, representing the weight of the edge among agents i and j, will be designed as a function of $d_{i1}, \ldots, d_{iN}$, $d_{j1}, \ldots, d_{jN}$, d_{ijo}, where $d_{ij} = \|x_{ij}\|$ is the distance among agents i and j, and d_{ijo} the distance between the segment s_{ij} connecting x_i with x_j (their line-of-sight) and the closest obstacle point o_{ij} (see Fig. 5). The weights A_{ij} are defined as a product of terms which vanish whenever one of the three properties in Def. 2 is not fulfilled (see Fig. 7):

$$A_{ij} = a_{ij}b_{ij}c_ic_j, \qquad c_i = \prod_{k|d_{ik}\leq D} c_{ik}, \tag{22}$$

with $a_{ij}(d_{ij})$ accounting for the constraint on inter-robot maximum sensing range D, $b_{ij}(d_{ijo})$ for the constraint on line-of-sight/obstacle distance (and implicitly for obstacle avoidance), and the $c_{ik}(d_{ik})$ accounting for the constraint on inter-robot minimum distances (i.e., to avoid inter-agent collisions).

The weights a_{ij} are chosen to stay constant at a maximum value k_a for $0 \leq d_{ij} \leq d_0$, where $0 < d_0 < D$ is a desired inter-robot distance, and to smoothly vanish (with vanishing derivative) if $d_{ij} = D$. Figure 6a shows the shape of a_{ij} for $d_0 = 4$, $D = 6$, and $k_a = 10$. As for b_{ij}, assume a minimum and maximum distance $0 \leq d^o_{\min} < d^o_{\max} \leq D$ between the segment s_{ij} and o_{ij} are chosen: Fig. 6b shows the shape of b_{ij} for $d^o_{\min} = 2$, $d^o_{\max} = 4$, and $k_b = 10$. Finally, weights c_{ik} are defined as being constant at a value k_c if $d_{ik} \geq d_0$, and to vanish, with vanishing derivative, for $d_{ik} = d_{\min}$, where $0 < d_{\min} < d_0$ represents a minimum desired distance between the agents. The shape of c_{ik} is conceptually the same as of b_{ij}, so we refer again the reader to Fig. 6b.

Notice that, because of (22) and the previous definitions, if agent i gets too close to an obstacle or to another agent, the entire i-th row of A will vanish, i.e., $A_{ij} = 0$, $\forall j$. Agent i would then become disconnected from the rest group, and any action aimed at preserving the connectivity would automatically enforce both obstacle and inter-agent collision avoidance.

Now consider the *Laplacian matrix* $L = diag(\delta_i) - A$, $\delta_i = \sum_{j=1}^{N} A_{ij}$, associated to the graph $\mathcal{G}$. It is well known that a measure of the connectivity of $\mathcal{G}$ is given by $\lambda_2 \geq 0$, the second smallest eigenvalue of L: $\lambda_2 > 0$ iff the graph is connected [29]. Since $A \in \mathcal{C}^1$, its eigenvalue λ_2 will be a differentiable function of d_{ij} and d_{ijo} for all the pair of agents, and will smoothly vanish as the graph approaches disconnection. It is then possible to build the potential function V^{λ} described in Sect. III as a function of λ_2 and try to follow the gradient of this potential to keep $\lambda_2 > 0$ at all times. For further details on this potential function and its 'i-th agent gradient' F^{λ}_i, we refer the reader to [21].

In particular, in [21] we shown that, apart from the (global) quantities λ_2 and ν_2 (the eigenvector associated to λ_2), F^{λ}_i can be evaluated locally since it only depends on the relative measurements d_{ij}, and d_{ijo}, $j \in \mathcal{N}_i$. Knowledge of λ_2 and ν_2 could be obtained by a global observation of the group in order to recover the full Laplacian L. However, we chose to rely on the decentralized estimation strategy proposed in by Yang *et al.* in [29]. Therein, the authors show how each agent i can obtain its own local estimation of λ_2, i.e., $\hat{\lambda}_2$, and of the i-th component of ν_2, i.e., $\hat{\nu}_{2_i}$, by again exploiting only local and 1-hop information. We refer the reader to this work for all the details.

Therefore, by exploiting these results, an estimation $\hat{F}^{\lambda}_i$ of the true F^{λ}_i can be implemented by every agent in a fully decentralized way. The main features of the potential V^{λ} and of F^{λ}_i introduced so far can be summarized as follows:

1) although V^{λ} is a global potential, reflecting global properties (connectivity) of the group, an estimation of $\hat{F}^{\lambda}_i$ can be computed in a fully decentralized way;
2) V^{λ} will grow unbounded as $\lambda_2 \to \lambda_2^{\min} > 0$, thus enforcing connectivity of the group. Note that, during the motion, agents are fully allowed to break or create links as long as $\lambda_2 > \lambda_2^{\min}$. This provides large amounts of flexibility to the group topology and geometry;
3) because of the shape of the terms a_{ij} and c_{ik}, $k \in \mathcal{N}_i$, minimization of V^{λ} will lead the agents i and j to keep a preferred inter-distance d_0, without getting too far or

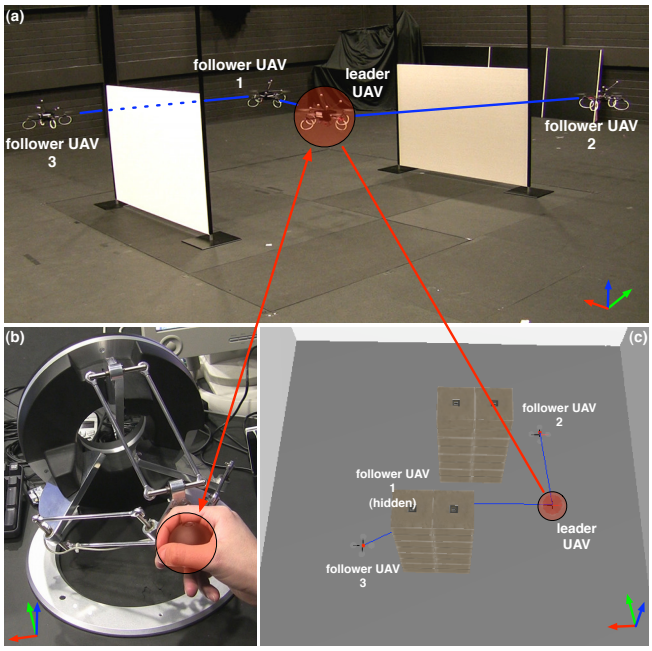

Fig. 8: The experimental setup.

too close to each other, since in either cases their link would approach disconnection resulting in a decrease of λ_2. Similarly, because of the shape and definition of b_{ij}, each pair of neighbors will try to keep its line-of-sight not occluded by obstacles;

4) because of the term $c_i c_j$ in (22), $\lambda_2 \to \lambda_2^{\min}$ as any inter-agent distance $d_{ij} \to d_{\min}$. Indeed, as an agent i approaches an agent j, the corresponding weight c_{ij} will vanish, implying that $A_{ik} \to 0 \; \forall k \in \mathcal{N}_i$ (since the same weight c_{ij} is present in all the A_{ik}, $k \in \mathcal{N}_i$). Agent i will loose all its links with the other agents and become disconnected from the group. Therefore, minimization of V^λ will prevent any inter-agent collision;
5) similarly to the previous case, because of the terms b_{ij}, any collision among agents and obstacles would imply $\lambda_2 \to \lambda_2^{\min}$ and, therefore, an unbounded growth of V^λ. As an agent i approaches an obstacle it will eventually become the closest point to the obstacle on all the links departing from it, i.e., on all the s_{ik}, $k \in \mathcal{N}_i$. At the minimum distance $d^o_{\min}$, all the b_{ik}, $k \in \mathcal{N}_i$, would vanish, leading to a disconnection of agent i from the rest of group like in the previous case.

Note that estimation errors in $\hat{F}_i^\lambda$ can potentially lead to a loss of passivity for the overall slave-side. However, it is again possible to exploit the tank reservoirs to 'passify' these shortcomings and obtain the desired passive behavior for the slave-side (formally, this is obtained by setting $w_i = -\beta_i \hat{F}_i^\lambda / x_{t_i}$ in (18)). See again [21] for all the details.

VIII. EXPERIMENTAL SETUP

A picture representing our experimental setup is shown in Fig 8. The master side consists of a 3-DOF force-feedback device, the Omega.3[5] (Fig. 8a), controlled via usb by a C++ program running on a dedicated GNU-Linux machine. This includes two threads: the first thread runs a synchronous loop at 2.5 KHz which accesses the current master position/velocity and sets the desired force F_m in (13). The second thread, running at a slower rate (125 Hz), acts as a network interface with the leader agent by exchanging the leader speed v_1 and the master command r_M.

The slave side is composed of 4 quadcopters[6] equipped with an embedded ATmega microprocessor and a standard integrated IMU (Fig. 8b). The microprocessor implements a low-level PID attitude controller by estimating the current attitude from the IMU measurements (via a complementary filter), and by controlling the pitch, roll, thrust and yaw-rate dofs of the UAV. This PID controller runs at about 450 Hz. Every quadcopter is also equipped with an additional Qseven single-board GNU-Linux machine[7] running a C++ program which implements a higher-level cartesian-control module: this computes the desired attitude and thrust commands and sends them to the low-level microprocessor via a serial interface whose baud rate is set to 115200. The Qseven board is also in charge of (1) communicating with the other UAVs via wireless ethernet, (2) communicating with the master device via wireless ethernet (only for the leader case), (3) implementing the inter-agent behavior described in the previous Sections, and (4) retrieving the current UAV position (and numerically estimating its velocity) from an external tracking system — the VICON system[8]. All the ethernet communication is implemented with the UDP protocol.

Finally, the detection of obstacles in the environment is simulated by means of a custom-made simulation environment based on the OGRE3D[9] engine (Fig. 8c). This runs on a separated machine connected to the same ethernet network of the UAVs from which it receives the corresponding (tracked) positions, and to which it sends back the surrounding obstacle points.

We have successfully run a number of hardware-in-the-loop simulations and real experiments with this setup to experimentally verify the theory summarized in this note. The interested reader is referred to our previous works [8, 22, 21] for any detail, and to our YouTube channel http://www.youtube.com/user/MPIRobotics for videos accompanying these experiments.

IX. CONCLUSIONS

In this paper, we have summarized our recent results [8, 21, 22] on the novel field of *Distributed Aerial Teleoperation* from a *bottom-up* perspective. The proposed theoretical framework, grounded on passivity-based control and port-Hamiltonian modeling, allowed large amounts of flexibility to the UAV fleet: the formation shape and topology can be autonomously adapt online via local split and join decisions due to sensing

[5] http://www.forcedimension.com
[6] http://www.mikrokopter.com
[7] http://www.seco.it
[8] http://www.vicon.com
[9] http://www.ogre3d.org/

and local task constraints, while 1) avoiding inter-agent and obstacle collisions, and 2) collectively following the human commands. Following our modeling and control framework, we were able to enforce passivity of the slave-side despite time-varying topology, to prove steady-state velocity synchronization among UAVs and master commands, and to guarantee connectivity maintenance despite the underlying time-varying interaction graph. A number of hardware-in-the-loop simulations and real experiments were also successfully run to validate our approach.

In the future, we aim at running a comparative analysis of the techniques available in the single-master single slave teleoperation (e.g., wave variables) for determining which one can be better adapted to the proposed multi-slave scenario. Furthermore, we would like to consider more leaders at the slave side in order to have a better control of the motion of the UAVs. Finally, we also plan to passively implement some extra forces at the master side in order to convey some extra information about the connectivity and for improving the telepresence feeling of the user.

For the interested reader, we also note that a complementary treatment of a related *top-down* approach [7, 9, 12] is reviewed and summarized in [6].

ACKNOWLEDGEMENTS

This research was partly supported by WCU (World Class University) program funded by the Ministry of Education, Science and Technology through the National Research Foundation of Korea (R31-10008).

REFERENCES

[1] A.Rahmani, M. Ji, M. Mesbahi, and M. Egerstedt. Controllability of multi-agent systems from a graph-theoretic perspective. *SIAM Journal on Control and Optimization*, 48(1):162–186, 2009.

[2] Y. Cao and W. Ren. Distributed coordinated tracking via a variable structure approach – part I: consensus tracking. part II: swarm tracking. In *American Control Conference*, pages 4744–4755, 2010.

[3] N. Chopra, M.W. Spong, and R. Lozano. Synchronization of bilateral teleoperators with time delay. *Automatica*, 44: 2142–2148, 2008.

[4] J. A. Fax and R. M. Murray. Information flow and cooperative control of vehicle formations. *IEEE Trans. on Automatic Control*, 9(3):1465–1476, 2004.

[5] J. Fink, N. Michael, S. Kim, and V. Kumar. Planning and control for cooperative manipulation and transportation with aerial robots. *International Journal of Robotics Research*, 30(3), 2010.

[6] A. Franchi. Decentralized bilateral aerial teleoperation of multiple uavs – Part II: a top-down perspective. In *Proc. of the 2011 RSS Workshop "3D Exploration, Mapping, and Surveillance with Aerial Robots"*, 2011.

[7] A. Franchi, C. Masone, H. H. Bülthoff, , and P. Robuffo Giordano. Decentralized bearing-only formation control for the bilateral teleoperation of multiple UAVs – Part I: Theory. In *submitted to 2011 IEEE/RSJ Int. Conf. on Intelligent Robots and Systems*, 2011.

[8] A. Franchi, P. Robuffo Giordano, C. Secchi, H. I. Son, and H. H. Bülthoff. A passivity-based decentralized approach for the bilateral teleoperation of a group of UAVs with switching topology. In *2011 IEEE Int. Conf. on Robotics and Automation*, Shangai, China, May Shanghai.

[9] V. Grabe, C. Masone, M. Ryll, A. Franchi, H. H. Bülthoff, and P. Robuffo Giordano. Decentralized bearing-only formation control for the bilateral teleoperation of multiple UAVs – Part II: Experiments. In *submitted to 2011 IEEE/RSJ Int. Conf. on Intelligent Robots and Systems*, 2011.

[10] A. Howard, L. E. Parker, and G. S. Sukhatme. Experiments with a large heterogeneous mobile robot team: Exploration, mapping, deployment and detection. *International Journal of Robotics Research*, 25(5-6):431–447, 2006.

[11] M. Ji and M. Egerstedt. Distributed coordination control of multiagent systems while preserving connectedness. *IEEE Trans. on Robotics*, 2007.

[12] D. Lee, A. Franchi, P. Robuffo Giordano, H. I. Son, and H. H. Bülthoff. Haptic teleoperation of multiple unmanned aerial vehicles over the internet. In *2011 IEEE Int. Conf. on Robotics and Automation*, Shanghai, China, May 2011.

[13] D. J. Lee and D. Xu. Feedback r-Passivity of Lagrangian Systems for Mobile Robot Teleoperation. In *2011 IEEE Int. Conf. on Robotics and Automation*, Shanghai, China, May 2011.

[14] N. E. Leonard and E. Fiorelli. Virtual leaders, artificial potentials and coordinated control of groups. In *40th IEEE Conf. on Decision and Control*, pages 2968–2973, Orlando, FL, Dec. 2001.

[15] S. Martinez, F. Bullo, J. Cortes, and E. Frazzoli. On synchronous robotic networks - Part II: Time complexity of rendezvous and deployment algorithms. *IEEE Trans. on Automatic Control*, 52(12):2214–2226, 2007.

[16] R. M. Murray. Recent research in cooperative control of multi-vehicle systems. *ASME Journal on Dynamic Systems, Measurement, and Control*, 129(5):571–583, 2007.

[17] G. Niemeyer and J.-J Slotine. Telemanipulation with time delays. *International Journal of Robotics Research*, 23 (9):873–890, 2004.

[18] G. Notarstefano, K. Savla, F. Bullo, and A. Jadbabaie. Maintaining limited–range connectivity among second–order agents. In *American Control Conference*, pages 2134–2129, 2006.

[19] L. C. A. Pimenta, V. Kumar, R. C. Mesquita, and G. A. S. Pereira. Sensing and coverage for a network of heterogeneous robots. In *47th IEEE Conf. on Decision and Control*, pages 3947–3952, Cancun, Mexico, Dec. 2008.

[20] W. Ren, R.W. Beard, and E.M. Atkins. Information

consensus in multivehicle cooperative control. *IEEE Control Systems Magazine*, 27(2):71 –82, 2007.

[21] P. Robuffo Giordano, A. Franchi, and C. Secchi H. H. Bülthoff. Bilateral teleoperation of groups of UAVs with decentralized connectivity maintenance. In *2011 Robotics: Science and Systems*, 2011.

[22] P. Robuffo Giordano, A. Franchi, C. Secchi, and H. H. Bülthoff. Experiments of passivity-based bilateral aerial teleoperation of a group of UAVs with decentralized velocity synchronization. In *submitted to 2011 IEEE/RSJ Int. Conf. on Intelligent Robots and Systems*, 2011.

[23] E. J. Rodriguez-Seda, J. J. Troy, C. A. Erignac, P. Murray, D. M. Stipanovic, and M. W. Spong. Bilateral teleoperation of multiple mobile agents: Coordinated motion and collision avoidance. *IEEE Trans. on Control Systems Technology*, 18(4):984–992, 2009. ISSN 1063-6536.

[24] M. Schwager, D. Rus, and J. J. Slotine. Decentralized adaptive coverage control for networked robots. *International Journal of Robotics Research*, 28(3):357–375, 2009.

[25] C. Secchi and C. Fantuzzi. Formation control over delayed communication networks. In *2008 IEEE Int. Conf. on Robotics and Automation*, pages 563–568, Pasadena, CA, May 2008.

[26] C. Secchi, S. Stramigioli, and C. Fantuzzi. *Control of Interactive Robotic Interfaces: a port-Hamiltonian Approach*. Springer Tracts in Advanced Robotics. Springer, 2007.

[27] H. I. Son, L. L. Chuang, A. Franchi, J. Kim, D. J. Lee, S. W. Lee, H. H. Bülthoff, and P. Robuffo Giordano. Measuring an operator's maneuverability performance in the haptic teleoperation of multiple robots. In *Submitted to 2011 IEEE/RSJ Int. Conf. on Intelligent Robots and Systems*, San Francisco, CA, Sep. 2011.

[28] H. I. Son, J. Kim, L. Chuang, A. Franchi, P. Robuffo Giordano, D. Lee, and H. H. Bülthoff. An evaluation of haptic cues on the tele-operator's perceptual awareness of multiple UAVs' environments. In *IEEE World Haptics Conference*, Istanbul, Turkey, Jun. 2011.

[29] P. Yang, R. A. Freeman, G. J. Gordon, K. M. Lynch, S. S. Srinivasa, and R. Sukthankar. Decentralized estimation and control of graph connectivity for mobile sensor networks. *Automatica*, 46:390–396, 2010.

[30] P. Yang, R. A. Freeman, and K. M. Lynch. Multi-agent coordination by decentralized estimation and control. *IEEE Trans. on Automatic Control*, 253(11):2480–2496, 2008.

[31] M. M. Zavlanos and G. J. Pappas. Potential fields for maintaining connectivity of mobile networks. *IEEE Trans. on Robotics*, 23(4):812–816, 2007.